Available online at www.sciencedirect.com
SCIENCE DIRECT®
Journal of Power Sources 141 (2005) 298–306
JOURNAL OF POWER SOURCES
www.elsevier.com/locate/jpowsour

Calendar life performance of pouch lithium-ion cells

Ramaraja P. Ramasamy, Ralph E. White, Branko N. Popov*

Department of Chemical Engineering, University of South Carolina, Columbia, SC 29208, USA

Received 18 September 2004; accepted 29 September 2004
Available online 7 December 2004

Abstract

An accelerated method was used to determine the effect of temperature, end-of-charge voltage and the type of storage condition over the performance pouch lithium-ion cells. The cells were studied for 4.0 V and 4.2 V end-of-charge voltages (EOCV) both at 5 °C and 35 °C. The irreversible capacity loss of the cell was analyzed every month using a capacity measurement protocol. The results indicated that higher temperature and voltage accelerates the degradation of the cells. The open circuit voltage (OCV) decay of the cells stored under open circuit conditions was also analyzed. The reasons for the irreversible capacity loss, energy loss, OCV decay and the increase in the internal resistance of the cell are discussed in detail. The most detrimental storage condition and the most mild storage condition are identified and discussed in detail.

Keywords: Aging; Storage life; Capacity loss; Lithium-ion; Open-circuit voltage

1. Introduction

It is essential to analyze the calendar life performance of batteries before they can be used in space applications where maintenance or replacement of batteries is practically impossible. Calendar life study can be defined as the test designed to evaluate cell degradation as a result of the passage of time with minimal usage [1]. It is not a pure shelf-life test, because the cells under test are periodically subjected to reference discharges to determine the changes (if any) in their performance characteristics.

There are a few studies, which describe the calendar life performance of lithium-ion batteries. Wright et al. [2] observed a square root of time dependence of resistance of the cells when they were stored for long period of time. Bloom et al. [3] observed area specific impedance increase and power fade in their accelerated calendar life studies on ATD Gen 1 lithium-ion cells. Jungst et al. [4] used neural network simulation approach to model the aging of lithium-ion batteries and observed a continuous increase in the impedance of the batteries with time. Asakura et al. [5] have studied the capacity retention of LP10 type lithium-ion batteries under float charging (FL) conditions. They observed capacity loss of 30% in 12 months at 45 °C even under mild conditions (float charging at 4.0 V) their batteries reached their end of life in 20 months.

The objective of this study was to analyze the effect of temperature, end-of-charge voltage (EOCV) and type of storage condition on the calendar life performance of lithium-ion cells. In our experiments, two different types of storage conditions namely float charging and open circuit (OC) conditions were studied. Both the self-discharge losses (OC) and also the losses that occur during continuous charging (FL) are analyzed. The data collected in this study are used to develop semi-empirical and first principles models, which will predict the self-discharge of these batteries as functions of temperature and end-of-charge voltage (state-of-charge, SOC).

2. Experimental

All experiments were performed on pouch lithium-ion batteries with name plate capacity of 1.67 Ah. All current rates (*C* rates) used in this study are based on the name plate ca-

* Corresponding author. Tel.: +1 803 777 7314; fax: +1 803 777 8265.
E-mail address: popov@engr.sc.edu (B.N. Popov).

0378-7753/$ – see front matter © 2004 Elsevier B.V. All rights reserved.
doi:10.1016/j.jpowsour.2004.09.024

Nomenclature

D_s	solid state diffusion coefficient
D_S^0	Arrhenius constant for diffusivity
E_a	apparent activation energy
E_{chg}	total charge energy
$E_{CC\text{-}chg}$	energy obtained during constant current charging
$E_{CV\text{-}chg}$	energy obtained during constant voltage charging
E_{dischg}	total discharge energy
E_0	equilibrium cell voltage
I	applied current
R	universal gas constant
R_S	sum of the ohmic and electrolyte resistances of the cell
R_P	polarization resistance of the cell
R_1	resistance of the anode
R_2	resistance of the cathode
T	temperature
Δt	time interval
V	cell voltage

Subscripts

i	time step
N	month number

pacity of the battery. The operating conditions are presented in Fig. 1a. The storage studies were done at two different temperatures namely at 5 °C and 35 °C, two different storage conditions, at float charge and at open circuit and for two different end-of-charge voltages. As shown in Fig. 1a, there are eight different storage conditions. Two cells were tested under each condition to ensure reproducibility. The storage experiments were performed by using an Arbin battery cycler. All cells were kept inside two Tenney environmental chambers at 5 °C and 35 °C, respectively. The humidity level inside the chambers was maintained at 0%.

Initially, before the commencement of storage experiments, the actual capacity of the cells was determined at 25 °C and used as a reference point in analyzing the storage data. The capacity was measured using the following procedure: to estimate the residual capacity remaining in the cell, the cells were discharged from their existing state-of-charge to 3 V using *C*/2 rate. The '*C*' rates were based on the name plate capacity of the cell (1.67 Ah, i.e. C_{rate} = 1.67 A). The cells were then charged to 4.2 V using *C*/5 rate. Next, the cells were kept at 4.2 V (CV charging mode) until the current decreased to 50 mA. The sum of the capacities obtained during both constant current (CC) and constant voltage (CV) steps is termed the charge capacity of the cell. The charged cells were then discharged to 3.0 V using *C*/2 rate. The capacity estimated during this step was termed the actual discharge capacity of the cell.

After the capacity measurement experiments, the temperature of the environmental chambers were set to 5 °C and 35 °C. The cells were charged using *C*/5 rate to their corresponding EOCVs. Once the cells reach their EOCVs, those cells that were to be float charged were maintained potentiostatic at the same EOCV (4.2 V or 4.0 V). The cells to be stored under open circuit conditions were kept at rest (open circuit). The storage experiments were conducted for a period of 30 days. At the end of 30 days, the storage studies were stopped and the temperature of the environmental chambers was set back to 25 °C. Next the capacity measurement procedure was repeated (using the same protocol as discussed above) to determine the actual capacity available in the cells after one month of storage. The conceptual test condition for *n*th month is shown in Fig. 1b. After the completion of capacity measurement for that month the storage studies were resumed by charging the cells to corresponding EOCV at the two different temperatures.

Electrochemical impedance spectroscopic (EIS) studies were conducted on one cell from each operating condition. The EIS studies were conducted after the capacity measurement procedure at the end of each month at 25 °C. Impedance experiments were also conducted initially before the commencement of the storage studies. The equipment used was a Solatron SI 1255 high frequency analyzer coupled with Princeton EG&G Model 273A potentiostat. Corrware and Z-plot software (Scriber Associates Inc.) was used to run the impedance experiments. The amplitude of the input AC signal was ±5 mV and the frequency range was between 10 kHz and 10 mHz.

3. Results and discussion

3.1. Data analysis

The actual discharge capacity is determined every month in the capacity measurement experiments. Due to irreversible capacity loss during storage, the actual capacity of the cell decreases every month (30 days). The irreversible capacity loss after '*N*' number of months is calculated as

$$\text{Irreversible capacity loss}|_N(\%) = \frac{\text{initial capacity} - \text{actual capacity}|_N}{\text{initial capacity}} \times 100$$

3.2. Discharge profiles

Fig. 2 shows typical discharge and charge profiles of the cell. The profiles were obtained during the initial capacity check experiments before the commencement of the calendar life studies. Both the charge and discharge studies were performed at 25 °C. The current rates used to charge and

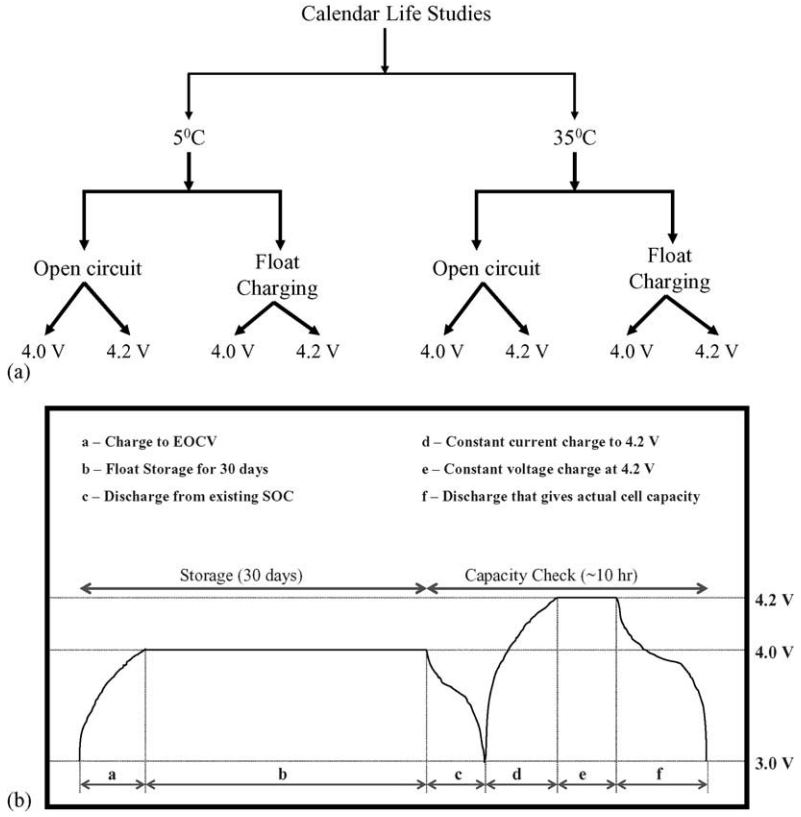

Fig. 1. (a) Schematic showing the various operating conditions used for storage studies. (b) Conceptual test conditions shown for *n*th month for the case of Float charging at 4.0 V EOCV.

discharge the cell are discussed above in the experimental section of this paper. The hump seen at 4.0 V in the profiles is characteristic of the $LiCoO_2$ material. The figure shows a flat plateau at 3.8 V. Experimentally, all the cells yielded a capacity of 2.2 Ah. As shown in Fig. 2, the cell is electrochemically reversible only in the range between 3.5 V and 4.2 V and does not deliver any useful energy below 3.5 V. The cell charges most of the time in constant current mode.

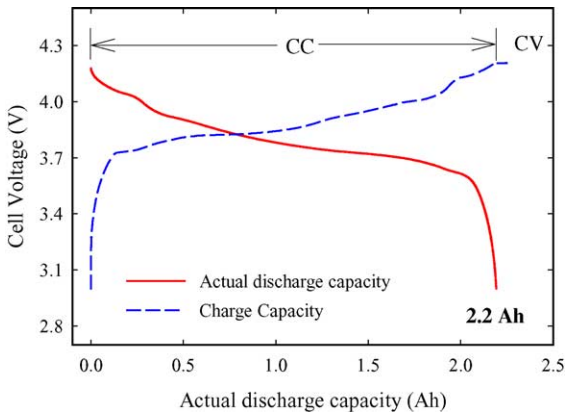

Fig. 2. Typical charge and discharge profiles obtained in the initial month before storage.

Initially less than 6% of the cell capacity is obtained under constant voltage charging.

The discharge profiles obtained after 6 months of storage are given in Fig. 3a and b. The initial discharge profile of the cell is also shown in the same figures for comparison. A notable difference can be seen in the shape of the profiles for the cells stored under both FL (Fig. 3a) and OC (Fig. 3b) storage conditions. The cells stored at 35 °C show a larger capacity loss than the cells stored at 5 °C under both storage conditions (FL and OC). Similarly the cells charged at higher EOCVs show a larger capacity loss. Two factors contribute to the shape change of the discharge profiles after 6 months of storage: the loss of active lithium-ions which result in the irreversible capacity loss of the cells that shifts the profile towards lower discharge capacity and the drop in the voltage plateau caused by the increase in the internal resistance of the cell. The internal resistance of the cell increases due to the surface film formed by the side reaction products. The term ‘side reaction’ indicates the parasitic reactions between the electrolyte and reversible lithium, which forms complex organic products that are electrochemically inactive. Side reactions occur on both electrodes but predominantly on the surface of the negative electrode [6]. Some examples of side reactions include reduction or organic solvent, decomposition of salt and dissolution of electrode material [7].

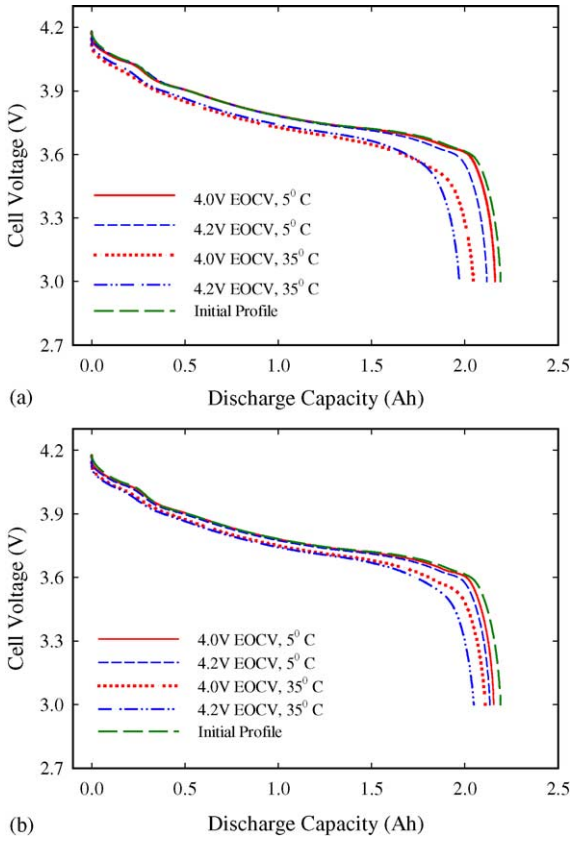

Fig. 3. Discharge profiles of the cells after 6 months of storage for (a) float charging storage conditions and (b) open circuit storage conditions.

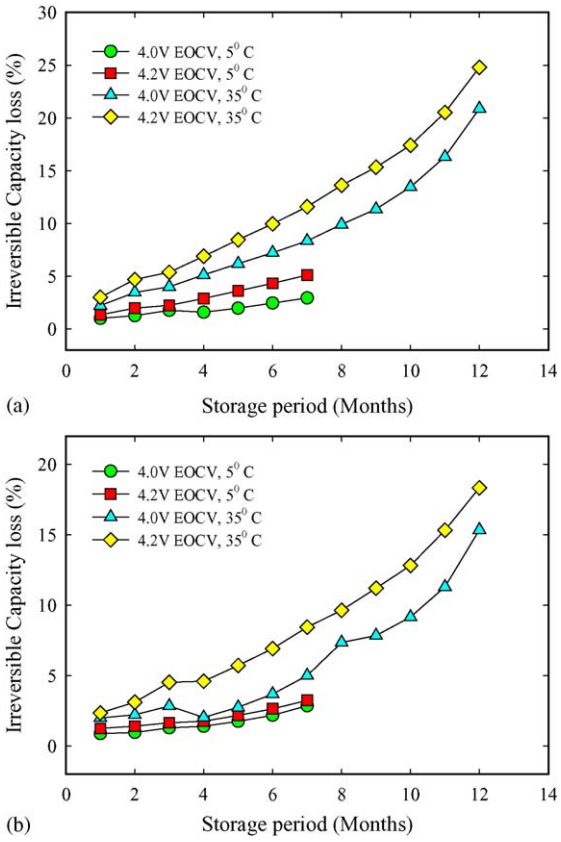

Fig. 5. Irreversible capacity loss of the cells for (a) float charging storage conditions and (b) open circuit storage conditions.

Fig. 4 shows discharge curves obtained after 1 year of storage at 35 °C under different storage conditions. The cells stored under open circuit conditions show less capacity loss than those stored under float potentials. The results indicate that higher temperature, higher EOCV and float potential storage result in a larger capacity loss.

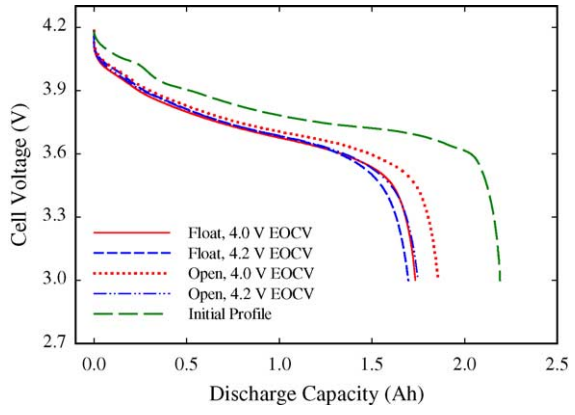

Fig. 4. Discharge profiles of the cells stored at 35 °C after 1 year of storage.

3.3. Irreversible capacity loss

The irreversible capacity losses at the end of each month are presented in Fig. 5a and b. Data are available for 7 months for the case of 5 °C and for 12 months for the case of 35 °C. Fig. 5a shows the irreversible capacity loss as a function of the storage time for cells stored under FL storage conditions. As shown in this figure, a steady increase in the capacity loss during each month is observed for all conditions. Cells stored at 35 °C consistently showed higher losses and similarly, cells stored at the higher EOCV (4.2 V) showed larger capacity loss. The overpotential for the side reactions occurring on the surface of the negative electrode is higher for higher EOCVs. Hence, the side reactions occur at a faster rate for higher EOCV (4.2 V) than the lower EOCV (4.0 V). Similar behavior can be seen for the cells stored under OC conditions shown in Fig. 5b. In the case of 35 °C, one observes an increase in the slope of the curves after 8 months of storage for both FL and OC conditions. This means that after 8 months of storage at 35 °C, the irreversible capacity loss increases at a faster rate than before. The results obtained are comparable with the results obtained by Asakura et al. [5]. They observed 18% and 30% capacity fade under continuous float charging conditions at 4.1 V at 25 °C and 45 °C, respectively. Under float storage at 4.2 V and at 45 °C, they observed

over 40% capacity fade in 12 months, which is much higher than the capacity fade observed in our studies.

3.4. OCV decay

The cells which were tested under OC conditions were kept at rest after they were charged to their corresponding EOCVs. The open circuit voltage (OCV) of these cells was monitored as a function of time for a period of 30 days until the next turn for the capacity check. As shown in Fig. 6, the open circuit voltage of the cells decreases continuously until it reaches an equilibrium value. The sudden voltage drop observed in Fig. 6 (shown only for 35 °C) during the first few hundred milliseconds is due to the internal cell resistance. After the ohmic drop region, the open circuit voltage of the cell decreases gradually as shown in the figure. The decrease in the cell voltage can be explained by taking into account the backdiffusion of lithium-ions from the surface of the negative electrode. When the cells are open-circuited, the lithium-ions at the surface of the negative electrode lose the driving force for diffusion in the solid phase. The lithium-ions backdiffuse into the electrolyte where they react with the solvent and form electron–ion–solvent complex [8]. Formation of the electron–ion–solvent complex is a self-discharge mechanism, which consumes active lithium-ions. Loss of active lithium-ions due to self-discharge decreases the solid phase concentration of the negative electrode thus increasing the potential of the carbon electrode in the positive direction [9]. This in turn decreases the overall cell voltage, which is reflected in Fig. 6.

The OCV decay of the cells is shown in Table 1. The OCP decay has been calculated as follows:

$$\text{OCV decay(V)} = \text{EOCV} - \text{cell voltage at the end of 30 days}$$

The table compares the OCV decay of all the four OC storage conditions during each month. We can analyze the effect of both EOCV and temperature on the OCV decay from this figure.

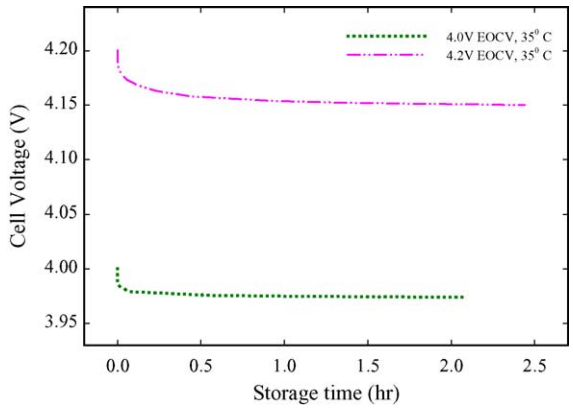

Fig. 6. A typical OCV decay curve showing the decrease in the OCV of the cells stored under open circuit storage conditions.

The reason for the larger difference in the values of OCV decay between 4.0 V and 4.2 V EOCVs at 5 °C can be explained based on the rate of diffusion of intercalation lithium-ions inside the solid bulk of the carbon electrode. It is a well-known fact that the carbon electrode has diffusion limitations. It is for this reason that the carbon electrode requires constant voltage charging in addition to the constant current charging to ensure complete charging of the cell. The rate of solid state diffusion is higher at high temperatures obeying the Eyring expression as below [10,11]

$$D_s = D_S^0 \exp\left(-\frac{E_a}{RT}\right)$$

where E_a is the apparent activation energy for the diffusion process, T the temperature, R the universal gas constant and D_S^0 is the Arrhenius constant for diffusivity. The intercalated lithium-ions will diffuse faster and in this way, at higher temperatures, solid phase concentration of lithium inside bulk of carbon particle increase at a faster rate than it does at lower temperatures. The increase in the solid phase concentration of lithium is directly reflected in the increase in the equilibrium potential of the cell. Hence, for a given EOCV, the cell gains more state-of-charge at higher temperature and hence attains higher equilibrium potentials. For the case of 35 °C, the cell attains higher equilibrium voltage even at lower EOCVs whereas at 5 °C, it requires higher EOCVs to attain higher equilibrium voltages. This is the reason for the large difference (60 mV) in the OCV decay values (see Table 1) between 4.0 V and 4.2 V EOCVs at 5 °C when compared to 35 °C (30 mV).

The highest OCV decay is observed for the cell stored at 5 °C with 4.2 V EOCV and the lowest value is for the cell stored at 35 °C with 4.0 V EOCV. The other two conditions show roughly the same values. The OCV decay continues to increase month-by-month due to the build-up of the internal resistance. This is explained in detail in the impedance studies

Table 1
OCV decay of the cells stored under OC conditions in 30 days for each month during the storage period

Month number	OCV decay			
	5 °C		35 °C	
	EOCV 4.0 V	EOCV 4.2 V	EOCV 4.0 V	EOCV 4.2 V
1	0.050	0.098	0.024	0.053
2	0.051	0.101	0.025	0.054
3	0.054	0.103	0.026	0.057
4	0.058	0.104	0.028	0.060
5	0.064	0.107	0.031	0.065
6	0.061	0.109	0.033	0.068
7	0.063	0.112	0.034	0.070
8			0.035	0.073
9			0.037	0.074
10			0.041	0.081
11			0.041	0.083
12			0.040	0.088

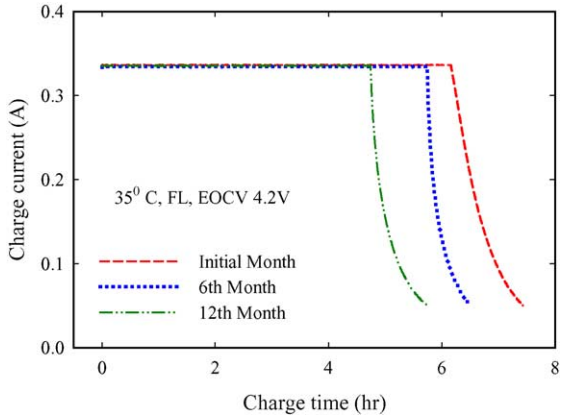

Fig. 7. Typical charge current profiles for the storage condition 35 °C, FL and 4.2 V EOCV.

discussed below. OCV decay has not heretofore been reported in literature.

3.5. Charge characteristics: cell capacity as a function of storage time

Fig. 7 shows the charge current profiles for the cell stored under FL conditions at 35 °C with EOCV of 4.2 V. The cells were charged by using a conventional CC/CV protocol. The capacity check measurements were conducted for a period of 6 and 12 months on cells stored at 5 °C and 35 °C. The horizontal line in Fig. 7 represents the CC charging time while the exponential regions represent the CV charging time. As shown in Fig. 7, the total charging time decreases when the storage time is increased, indicating that irreversible capacity loss has occurred in these cells. The duration of the total charging time (CC + CV) decreases from the initial charging time of 7.4 h to 5.7 h in 12 months. Table 2 compares both constant current and constant voltage times as a function of storage duration at two different temperatures. Initially as shown in Table 2, approximately 95% of the cell's capacity was charged in CC mode and less than 6% was charged in CV mode. This initial CC/CV ratio was the same for all storage conditions. However, upon storing the cells for a long period of time at different temperatures the ratio between CC and CV charge capacities changes considerably. As shown in the table, a continuous decrease in the CC charge capacity and simultaneously increase in the CV charge capacity occurs during storage. This is true for all eight storage conditions. The ratio of CC/CV charge capacities decreases faster at 35 °C than at 5 °C. It can also be noticed from the table that this ratio changes most for FL charging condition at 4.2 V EOCV and least for OC charging condition at 4.0 V EOCV.

Table 2
Percentages values of capacities charged in constant current (CC) and constant voltage (CV) modes for initial, 6th and 12th months

Storage condition	Duration (months)	5 °C		35 °C	
		CC (%)	CV (%)	CC (%)	CV (%)
Float, 4.0 V	Initial	96.1	3.9	94.0	6.0
	6	94.4	5.6	87.8	12.2
	12			84.7	15.3
Float, 4.2 V	Initial	94.6	5.4	93.9	6.1
	6	92.3	7.7	88.5	11.5
	12			82.8	17.2
Open, 4.0 V	Initial	95.0	5.0	94.1	5.9
	6	93.1	6.9	91.3	8.7
	12			87.6	12.4
Open, 4.2 V	Initial	95.2	4.8	94.1	5.9
	6	93.3	6.7	89.8	10.2
	12			85.3	14.7

The increase in the CV charging time and the decrease in the CC charging time may result from a decrease of the Li^+ ion transference number and increase in the internal resistance for Li-ion intercalation which is directly related to the rate capability of the cell [12]. The transference number of Li^+ decreases due to dissolution of corrosion and reaction by-products into the electrolyte. The corrosion products formed on the surface also increase mass transfer limitations for Li^+ intercalation. The increase in the internal cell resistance is attributed to the increase in the thickness of the surface film formed on both electrodes. The internal cell resistance continues to increase with time of storage. As a result the cell attains its EOCV faster when charged in CC charging mode. Detailed discussion of the internal cell resistance can be found in the impedance section of this paper.

3.6. Energy loss

The total energy (E) of a battery during complete charge or complete discharge can be estimated by summation of the product of cell voltage, current (during charge or discharge) and the time of charge/discharge. During charge, the battery is subjected to both constant current and constant voltage. The total energy obtained is the sum of the energy expended during these two portions of the charge curve. This can be calculated as

$$E_{\text{CC-chg}} = \sum_i V_i I \Delta t_i \quad (1)$$

$$E_{\text{CV-chg}} = \sum_i V I_i \Delta t_i \quad (2)$$

$$E_{\text{chg}} = E_{\text{CC-chg}} + E_{\text{CV-chg}} \quad (3)$$

where $E_{\text{CC-chg}}$ is the energy that the battery gains during constant current charging, during which the voltage rise is monitored for specific time intervals. The energy gains during the constant voltage $E_{\text{CV-chg}}$ charge could also be defined in the same way. The term Δt is the time interval used to log in the data. The summation of the energies of both CC and CV charging is the total charge energy, as given in (3). Similarly,

Table 3
Charge and discharge energies for all the eight storage conditions for various durations of storage.

Storage condition	Duration (months)	Charge energy (%)		Discharge energy (%)	
		5 °C	35 °C	5 °C	35 °C
Float, 4.0 V	Initial	100	100	100	100
	4	96.3	95.3	99.6	94.3
	6	95.5	93.1	98.7	91.4
	9		89.0		87.6
	12		80.5		77.4
Float, 4.2 V	Initial	100.0	100	100	100
	4	96.1	93.0	98.1	93.0
	6	94.6	90.0	96.7	89.7
	9		84.9		84.1
	12		77.2		75.8
Open, 4.0 V	Initial	100	100	100	100
	4	98.3	96.0	99.2	97.4
	6	97.3	94.2	98.3	95.4
	9		90.0		90.5
	12		84.2		83.2
Open, 4.2 V	Initial	100	100	100	100
	4	95.8	94.7	98.3	96.9
	6	94.7	92.2	97.2	92.5
	9		87.3		86.9
	12		79.3		78.1

the discharge energy can be calculated as

$$E_{\text{dischg}} = \sum_i V_i I \Delta t_i \tag{4}$$

The percentage energy loss is calculated in the same way as that of the irreversible capacity loss. The energy loss (for both charge energies and discharge energies) after '*N*' number of months is calculated as

$$\text{Energy loss}|_N(\%) = \frac{\text{initial energy} - \text{actual energy}|_N}{\text{initial energy}} \times 100 \tag{5}$$

The values of initial charge energy and initial discharge energy were 8.7 Wh and 8.3 Wh, respectively. The percentage charge and discharge energies as a function of storage time estimated at 5 °C and 35 °C for EOCV of 4.0 V and 4.2 V after complete charge and discharge are given in Table 3. The percentage values were calculated according to (5). As shown in Table 3, the charge energy decreases by 2–5% at 5 °C and by 16–23% at 35 °C. Similarly the discharge energy decrease by 2–4% at 5 °C after 6 months of storage and by 17–24% at 35 °C after 12 months of storage. The highest energy loss is observed for the FL condition at 35 °C with 4.2 V EOCV of 4.2 V (23% after 12 months) and the least energy loss is observed for the OC condition at 5 °C with 4.0 V EOCV (2% after 6 months). Although there is a loss in the total charge and discharge energies with storage, there is no significant change in the overall energy efficiency at both temperatures. The energy efficiency is the ratio of the discharge energy to charge energy. Energy efficiency of the cells decreased by less than 1% after 6 months for the cells stored at 5 °C. For the cells stored at 35 °C, this value is less than 2% even after 12 months of storage. However, lithium-ion batteries show higher energy loss when cycled at high temperatures [12].

3.7. Impedance measurements

In general the cell voltage of a Li-ion cell can be given as

$$V = E_0 - I(R_S + R_P)$$

where E_0 is the equilibrium cell voltage (OCV), I is the charging current, R_S is the sum of electrolyte and ohmic resistances of the cell and R_P is the time dependent polarization resistance which is the sum of the anode and the cathode resistances.

Electrochemical impedance spectroscopy was used to estimate the overall resistances of the cells. The measurements were done every month after capacity check measurements. Fig. 8 shows Nyquist plots of an MSA cell for the initial, 6th and 12th months. The plots were obtained at a frequency range between 25 Hz and 10 mHz. The overall cell impedance is the sum of the positive and negative electrode impedances and the solution resistance. It has been proved that the equivalent circuit shown in Fig. 8 can be used to fit the impedance date of the full cell [13]. The R_1C_1 and R_2C_2 components represent impedance on the cathode and anode side, respectively. Both anode and cathode impedances include several individual contributions in them. The individual contributions to the impedance of each electrode are migration resistance through the multilayer surface films and charge transfer resistance at the electrode-electrolyte interface on both electrodes. However, contribution from each of these resistances could be determined only by conducting EIS studies on individual electrodes (R_1 and R_2). The component R_S represents the solution resistance offered by the electrolyte. The intercept of the curve on the *x*-axis in the high frequency region can be attributed to R_S. The magnitude of the semi-circle in the

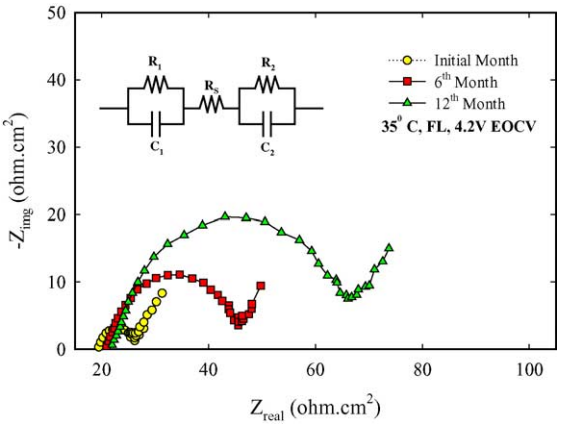

Fig. 8. Nyquist plots showing the increase in the impedance of the cell during storage at 35 °C float potential storage with 4.2 V EOCV.

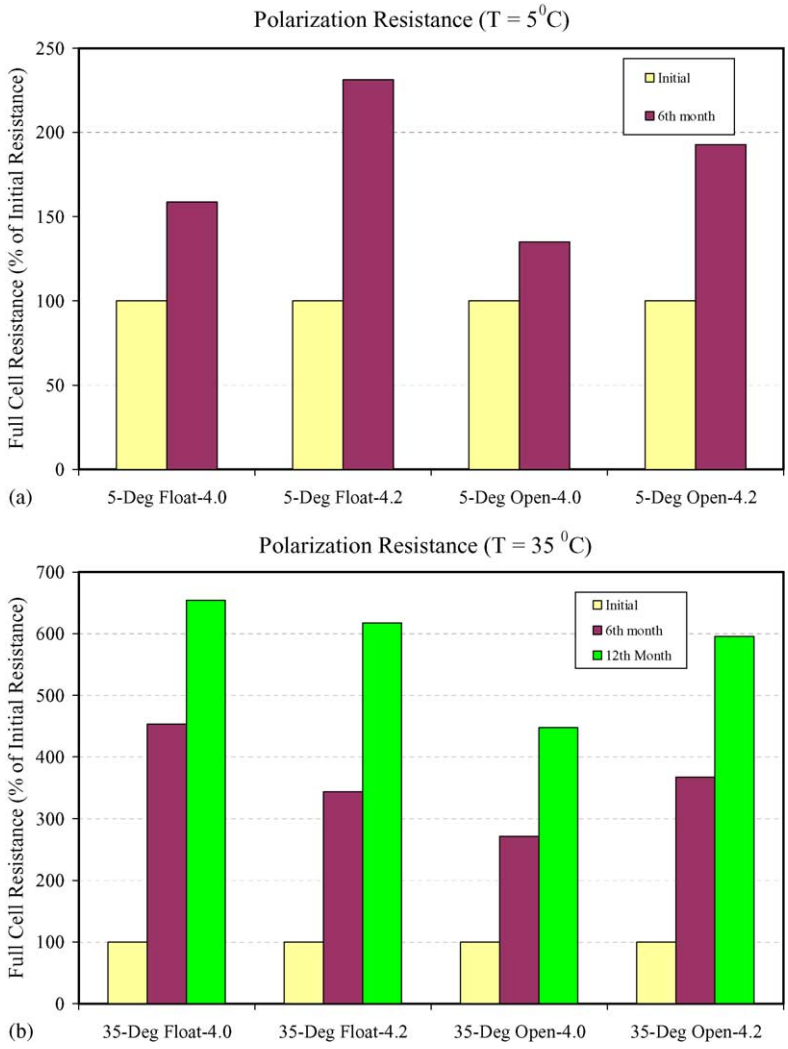

Fig. 9. Polarization resistances of the cell after 6 and 12 months of storage at (a) 5 °C and (b) 35 °C.

medium frequency region is directly related to the overall internal impedance of the cell. The overall internal impedance (polarization resistance) of the full cell is given by [13]

$$R_P = R_1 + R_2$$

The overall polarization resistance of the cell R_P can be taken equal to the diameter of the semi-circle occurring at the mid-frequency region. The increase in the internal cell impedance (R_P) with time of storage is given is Fig. 9a and b. Fig. 9a shows the value of impedance after 6 and 12 months. The percentage values are based on initial impedance of the cell for each storage condition. It can be observed from Fig. 9a and b that the internal cell resistance increases more rapidly for the FL charging conditions than the OC conditions. Moreover, higher EOCVs always increase the cell resistance rapidly. The exception for this is the FL condition at 35 °C. After 6 months of storage, the resistance increased by 3–4 times at 35 °C and only 1.5–2 times at 5 °C. This is because the impedance of the cell increases with increase in temperature [14]. High temperature is always detrimental to the lithium-ion cell because of the following: (1) decomposition/evaporation of electrolyte occurs at higher temperatures; (2) solvent reduction is predominant at higher temperatures over the surface of the negative electrode, which increases the thickness of the SEI film; (3) the electrode active material dissolves at high temperatures; and (4) formation of inactive oxides on the cathode and the rate of side reactions at the anode occur at much faster rate at higher temperatures.

4. Conclusion

The calendar life studies have shown that lithium-ion batteries exhibit a notable capacity loss during storage. The capacity loss has been found to increase continuously with storage time for all eight storage conditions. For the cells stored under open circuit conditions, the OCV of the cell decayed with time and the decay continues to increase with duration of storage. The largest capacity loss has been found for the cell stored under the FL condition at 35 °C with 4.2 V EOCV.

The least capacity loss has been observed for the cell stored under the OC condition at 5 °C with 4.0 V EOCV. In general, 35 °C is more detrimental to the cell than 5 °C because at higher temperatures, solvent oxidation and loss of lithium are greater than at lower temperatures. Higher EOCV (4.2 V) has been found to cause more capacity loss because of the higher overpotential for side reactions occurring at the surface of the negative electrode. It has also been found that the capacity loss is always larger for the float charging conditions than the open circuit conditions. The charge and discharge energies of the cells continue to decrease with time of storage for all eight conditions. The cells stored at 35 °C also show higher increase in internal resistance. More information regarding the resistance of the film formed on the electrodes, active material dissolution and phase transformation can be obtained by analyzing the individual electrodes taken out of the batteries after various periods of storage.

Acknowledgements

Financial support provided by National Reconnaissance Office is greatly acknowledged.

References

[1] PNGV Test Plan for ATD 18650 Gen 1 Lithium-Ion Cells, Revision 4, EHV-TP-103, December 1999.
[2] R.B. Wright, C.G. Motloch, J.R. Belt, J.P. Christophersen, C.D. Ho, R.A. Richardson, I. Bloom, S.A. Jones, V.S. Battaglia, G.L. Henriksen, T. Unkelhaeuser, D. Ingersoll, H.L. Case, S.A. Rogers, R.A. Sutula, J. Power Sources 110 (2) (2002) 445.
[3] I. Bloom, B.W. Cole, J.J. Sohn, S.A. Jones, E.G. Polzin, V.S. Battaglia, G.L. Henriksen, C. Motloch, R. Richardson, T. Unkelhaeuser, D. Ingersoll, H.L. Case, J. Power Sources 101 (2) (2001) 238.
[4] R.G. Jungst, G. Nagasubramanian, H.L. Case, B.Y. Liaw, A. Urbina, T.L. Paez, D.H. Doughty, J. Power Sources 119–121 (2003) 870.
[5] K. Asakura, M. Shimomura, T. Shodai, J. Power Sources 119–121 (2003) 902.
[6] P. Arora, R.E. White, M. Doyle, J. Electrochem. Soc. 145 (1998) 3647.
[7] D. Aurbach, E. Zinigrad, Y. Cohen, H. Teller, Solid State Ionics 148 (2002) 405.
[8] R. Yazami, Y.F. Reynier, Electrochim. Acta 47 (2002) 1217.
[9] C. Wang, X. Zhang, A.J. Appleby, X. Chen, F.E. Little, J. Power Sources 112 (1) (2002) 98.
[10] R.B. Bird, W.E. Stewart, E.N. Lightfoot, Transport Phenomena, second ed. (Chapter 17).
[11] J. Karger, D.M. Ruthven, Diffusion in Zeolites, Wiley, New York, 1992.
[12] P. Ramadass, B. Haran, R. White, B.N. Popov, J. Power Sources 112 (2) (2002) 606.
[13] D. Zhang, B.S. Haran, A. Durairajan, R.E. White, Y. Podrazhansky, B.N. Popov, J. Power Sources 91 (2000) 122.
[14] I. Bloom, S.A. Jones, E.G. Polzin, V.S. Battaglia, G.L. Henriksen, C.G. Motloch, R.B. Wright, R.G. Jungst, H.L. Case, D.H. Doughty, J. Power Sources 111 (1) (2002) 152.